[10] N. Sorensen and W. Ren, "A unified formation control scheme with a single or multiple leaders," in *Proc. Amer. Control Conf.*, New York, NY, Jul. 2007, pp. 5412–5418.
[11] G. Montemayor and J. T. Wen, "Decentralized collaborative load transport by multiple robots," in *Proc. IEEE Int. Conf. Robot. Autom.*, Barcelona, Spain, Apr. 2005, pp. 372–377.
[12] J. T. Wen and K. Kreutz-Delgado, "Motion and force control of multiple robotic manipulators," *Automatica*, vol. 28, no. 4, pp. 729–743, 1992.
[13] K. Munawar and M. Uchiyama, "Experimental verification of distributed event-based control of multiple unifunctional manipulators," in *Proc. IEEE Int. Conf. Robot. Autom.*, 1999, pp. 1213–1218.
[14] G. A. S. Pereira, V. Kumar, and M. F. M. Campos, "Decentralized algorithms for multirobot manipulation via caging," *Int. J. Robot. Res.*, vol. 23, pp. 783–795, 2002.
[15] Y. Zheng and Y. Luh, "Control of two coordinated robots in motion," in *Proc. 25th IEEE Conf. Decis. Control*, Ft. Lauderdale, FL, Dec. 1985, pp. 334–337.
[16] Y. Hirata, Y. Kume, Z. Wang, and K. Kosuge, "Decentralized control of multiple mobile manipulators handling a single object in coordination," in *Proc. IEEE Int. Conf. Intell. Robots Syst.*, Oct. 2002, pp. 2758–2763.
[17] C. P. Tang, R. M. Bhatt, M. Abou-Samah, and V. Krovi, "Screw-theoretic analysis framework for cooperative payload transport by mobile manipulator collectives," *IEEE/ASME Trans. Mechatron.*, vol. 11, no. 2, pp. 169–178, Apr. 2006.
[18] D. Sun and J. K. Mills, "Manipulating rigid payloads with multiple robots using compliant grippers," *IEEE/ASME Trans. Mechatron.*, vol. 7, no. 1, pp. 23–34, Mar. 2002.
[19] T. G. Sugar and V. Kumar, "Control of cooperating mobile manipulators," *IEEE Trans. Robot. Autom.*, vol. 18, no. 1, pp. 94–103, Feb. 2002.
[20] H. G. Tanner, K. J. Kyriakopoulos, and N. I. Krikelis, "Modeling of multiple manipulators handling a common deformable object," *J. Robot. Syst.*, vol. 15, no. 11, pp. 599–623, 1998.
[21] H. Bai, M. Arcak, and J. T. Wen, "Adaptive design for reference velocity recovery in motion coordination," *Syst. Control Lett.*, vol. 57, no. 8, pp. 602–610, 2008.
[22] H. Bai and J. T. Wen, "Motion coordination through cooperative payload transport," in *Proc. Amer. Control Conf.*, St. Louis, MO, Jun. 2009, pp. 1310–1315.

Sliding-Mode Velocity Control of Mobile-Wheeled Inverted-Pendulum Systems

Jian Huang, Zhi-Hong Guan, Takayuki Matsuno, Toshio Fukuda, and Kosuke Sekiyama

***Abstract*—There has been increasing interest in a type of underactuated mechanical systems, mobile-wheeled inverted-pendulum (MWIP) models, which are widely used in the field of autonomous robotics and intelligent vehicles. Robust-velocity-tracking problem of the MWIP systems is investigated in this study. In the velocity-control problem, model uncertainties accompany uncertain equilibriums, which make the controller design become more difficult. Two sliding-mode-control (SMC) methods are proposed for the systems, both of which are capable of handling both parameter uncertainties and external disturbances. The asymptotical stabilities of the corresponding closed-loop systems are achieved through the selection of sliding-surface parameters, which are based on some rules. There is still a steady tracking error when the first SMC controller is used. By assuming a novel sliding surface, the second SMC controller is designed to solve this problem. The effectiveness of the proposed methods is finally confirmed by the numerical simulations.**

***Index Terms*—Mobile-wheeled inverted pendulum (MWIP), robust control, sliding-mode control (SMC), stability, underactuated systems.**

I. Introduction

Recently, many investigations have been devoted to problems of controlling mobile-wheeled inverted pendulum (MWIP) models, which have been widely applied in the field of autonomous robotics and intelligent vehicles [1]–[12]. The MWIP models are not only of theoretical interest but are also of practical interest. Many practical systems have been implemented that were based on the MWIP models, such as the JOE [7], the Nbot [8], the Legway [9], the B2 [10], the Segway [11], etc. Among these applications, the Segway PT has been a popular personal transporter, since it was invented in 2001. Such systems are characterized by the ability to balance on its two wheels and spin on the spot. This additional maneuverability allows them to easily navigate on various terrains, turn sharp corners, and traverse small steps or curbs. In addition, the compact structure design allows drivers to access most places that can only be accessed by walkers in the past. Moreover, people can drive such vehicles to travel short distances in a small area instead of using cars or buggies that are more pollutive.

From the theoretical point of view, the MWIP models have attracted much attention in the field of control theory and engineering because

Manuscript received January 25, 2010; revised June 9, 2010; accepted June 9, 2010. Date of publication July 23, 2010; date of current version August 10, 2010. This paper was recommended for publication by Associate Editor T. Murphey and Editor J.-P. Laumond upon evaluation of the reviewers' comments. This work was supported by the National Natural Science Foundation of China under Grant 60603006 and Grant 60834002 and by the Doctoral Foundation of Ministry of Education of China under Grant 20090142110039.

J. Huang and Z.-H. Guan are with the Department of Control Science and Engineering, Huazhong University of Science and Technology, Wuhan 430074, China. They are also with the Key Laboratory for Image Processing and Intelligent Control of Education Ministry of China, Wuhan 430074, China (e-mail: huang_jan@mail.hust.edu.cn; zhguan@mail.hust.edu.cn).

T. Matsuno is with the Department of Intelligent System Design Engineering, Toyama Prefectural University, Imizu 939-0398, Japan (e-mail: matsuno@pu-toyama.ac.jp).

T. Fukuda and K. Sekiyama are with the Department of Micro-Nano Systems Engineering, Nagoya University, Nagoya 464-8603, Japan (e-mail: fukuda@mein.nagoya-u.ac.jp; sekiyama@robo.mein.nagoya-u.ac.jp).

Color versions of one or more of the figures in this paper are available online at http://ieeexplore.ieee.org.

Digital Object Identifier 10.1109/TRO.2010.2053732

they are nonlinear and underactuated with inherent unstable dynamics. Many control techniques have been studied in the past decades for the control of benchmark underactuated systems, such as the inverted pendulum, the Acrobot, and the rotating pendulum. A control technique that is composed of swing-up and balancing controller was designed with the use of partial feedback linearization to balance the pendulum [13]. Other methods, like passivity-based, adaptive, and controlled Lagrangians techniques, have also found their way into the control of underactuated mechanical systems [14]–[16]. Nevertheless, most of these methods are based on the exact mathematical models and lack of robustness to model errors and external disturbances. In the case of MWIP models, although they are essentially nonlinear and underactuated, most of the previous work used linear [2]–[5] or feedback linearization methods [1], [12] to model and control them. Linear-feedback controller of a nonlinear system might yields a small region of attraction, and it lacks robustness to parameter uncertainty. On the other hand, feedback linearization involves the exact cancellation of nonlinearities. Consequently, it relies on a rather precise description of nonlinear functions. $H\infty$ method has also been applied to control the B2 vehicle, although it is still based on a reference linear model, and only the balancing problem was investigated [17].

The sliding-mode control (SMC) might be a comparatively appropriate approach to deal with uncertain MWIP systems because SMC is less sensitive to the parameter variations and noise disturbances, whereas it is not easy to design SMC controllers for nonlinear underactuated systems, whose control problems have been proved to be challenging, because the techniques of fully actuated systems cannot be used directly. Wang proposed a hierarchical SMC method for a class of second-order underactuated systems [18]. Nevertheless, the results are still in dispute [19]. Ashrafiuon and Erwin proposed an SMC approach for underactuated multibody systems [20]. This approach was further applied into a robust-tracking-control problem of the biped robots [21]. In their study, more attention is paid to external disturbances than to the parameter uncertainty. As for the special cases of underactuated systems, Lee and Coverstone-Carroll [22] and Su and Stepanenko [23] applied the SMC methods to the robust control of the Acrobot and the underactuated manipulator, respectively. In [24], Huang *et al.* proposed an SMC control scheme, which is based on a novel sliding surface, to realize the velocity control of an MWIP system that suffers from uncertainties. More theoretical analyses and comparison study of performances for different SMC controllers will be presented in this paper.

In this paper, two new SMC approaches are proposed to realize the velocity-tracking problem of a mobile-wheeled inverted pendulum. Both model uncertainties and external disturbances are taken into account in the controller design. The rest of the paper is organized as follows. In Section II, the model formulation and equilibrium analysis are discussed. Section III describes the design procedure of the first SMC controller, which is robust, but with a steady tracking error. Section IV proposes the second SMC controller based on a novel sliding surface. By using this new SMC controller, the uncertain equilibrium problem is solved so that the steady tracking error can be removed. Finally, the effectiveness of the proposed methods is proved through numerical simulations.

II. System Formulation

A. Dynamic Model

The MWIP system is modeled as a one-dimensional (1-D) inverse pendulum that rotates about the wheels' axles. Hence, the body's motion on a plane is determined by the inclination and translational motion. Fig. 1 shows the structure of an MWIP system, where θ_w and θ_b are the wheel's rotation angle and the inclination angle of the body, respectively. The coordinates of the wheel and body are denoted by (x_w, y_w) and (x_b, y_b), respectively. We suppose that the system moves on a slope with constant, but uncertain angle α, which is hard to be measured by sensors. To describe the parameters of the MWIP system, some notations should be clarified first (see also Fig. 1), which are as follows:

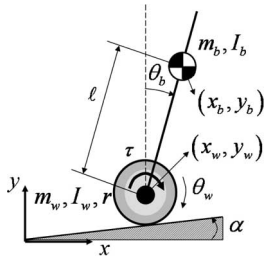

Fig. 1. Mobile-wheeled inverted-pendulum system model.

1) m_b, m_w masses of the body and the wheel;
2) I_b, I_w moments of inertia of the body and the wheel;
3) l length between the wheel axle and the center of gravity of the body;
4) r radius of the wheel;
5) D_b viscous resistance in the driving system;
6) D_w viscous resistance of the ground.

Lagrange's motion equation is used to analyze the dynamics of this system, which leads to a second-order underactuated model, which is given by

$$\begin{cases} m_{11}\ddot{\theta}_w + (m_{12}\cos(\theta_b+\alpha))\ddot{\theta}_b \\ \quad = \tau - D_w\dot{\theta}_w + D_b\left(\dot{\theta}_b - \dot{\theta}_w\right) + m_{12}\dot{\theta}_b^2\sin(\theta_b+\alpha) - \tilde{M} \\ (m_{12}\cos(\theta_b+\alpha))\ddot{\theta}_w + m_{22}\ddot{\theta}_b \\ \quad = -\tau - D_b\left(\dot{\theta}_b - \dot{\theta}_w\right) + G_b\sin\theta_b \end{cases} \tag{1}$$

where parameters m_{11}, m_{12}, m_{22}, and G_b satisfy

$$\begin{cases} m_{11} = (m_b + m_w)r^2 + I_w \\ m_{12} = m_b l r \\ m_{22} = m_b l^2 + I_b \\ G_b = m_b g l \\ \tilde{M} = (m_b + m_w) r g \sin\alpha. \end{cases} \tag{2}$$

The derivation of model (1) is given in the Appendix. As compared with the model presented in [26], we here ignore the mass of rotor and take the viscous resistance of ground into account, which is inevitable in the reality. In addition to the unknown slope angle α, other model uncertainties come from the body parameters m_b and I_b. For instance, if an MWIP model is used to describe a Segway vehicle, then the body is composed of the control shaft and the passenger. Because of the different weights of persons, body parameters m_b and I_b are apparently uncertain before the controller design. The aim of this study is to design a robust controller, which can make the vehicle to move at a desired velocity without steady error, as well as guarantee the system stability, even when there are model uncertainties and disturbances. It should be pointed out that only straight velocity-control problem is investigated here. Hence, 3-D model of the vehicle, as given in [1], is not required.

B. Analysis of Equilibriums

By choosing the state variable as $\mathbf{x} = [\,x_1 \quad x_2 \quad x_3\,]^T = [\,\theta_b \quad \dot{\theta}_w \quad \dot{\theta}_b\,]^T$, the state model of an MWIP system can be represented by

$$\mathbf{M}(\mathbf{x})\dot{\mathbf{x}} = \mathbf{F}(\mathbf{x}) + \mathbf{u} \tag{3}$$

where

$$\mathbf{M}(\mathbf{x}) = \begin{bmatrix} 1 & 0 & 0 \\ 0 & m_{11} & m_{12}\cos(x_1+\alpha) \\ 0 & m_{12}\cos(x_1+\alpha) & m_{22} \end{bmatrix}$$

$$\mathbf{F}(\mathbf{x}) = \begin{bmatrix} x_3 \\ -D_w x_2 + D_b(x_3 - x_2) + m_{12}x_3^2\sin(x_1+\alpha) - \tilde{M} \\ -D_b(x_3 - x_2) + G_b \sin x_1 \end{bmatrix}$$

$$\mathbf{u} = [\,0 \quad \tau \quad -\tau\,]^T.$$

Let us suppose that $\mathbf{x}^* = [\,x_1^* \quad x_2^* \quad x_3^*\,]^T$ is the desired equilibrium of the system (3) that satisfies

$$x_3^* = 0, \qquad G_b \sin x_1^* = D_w x_2^* + \tilde{M}. \tag{4}$$

In the case of a velocity-control problem, the desired velocity $\dot{\theta}_w^* = x_2^*$ is always given in advance. The desired inclination angle of the body x_1^* is then determined by (4), whereas different body parameters and unknown slope angle result in different inclination angle x_1^*, which makes it impossible to compute the exact equilibrium before the controller design. Normally, it is difficult to design a controller, if we do not know the exact equilibrium in advance. Especially, in the case of using a linearized model, we cannot even obtain such model because it is generated by linearization of the nonlinear system around the equilibrium. This problem can be partially solved by the estimation of the equilibrium by using nominal system parameters, without considering any uncertainties. Whereas the controller based on the estimated equilibrium cannot guarantee the system that finally moves at the desired velocity, even if it is asymptotically stable. This will be further discussed in the rest of paper.

In the rest of this paper, "^" denotes that the terms are evaluated based on parameters of the nominal system that moves on a flat ground with no uncertainties and disturbances.

III. Design of the First Sliding-Mode-Control Controller

A. Sliding-Mode Controller Design

We base our controller design on full-state feedback. The sliding surface is defined as a weighted combination of the position-tracking error and the velocity-tracking error, which is given by

$$s = \lambda_1 \tilde{x}_1 + \lambda_2 \tilde{x}_2 + \tilde{x}_3 \tag{5}$$

where $\tilde{x}_i = x_i - \hat{x}_i^*$ are the tracking errors with $i = 1, 2, 3$, and coefficients λ_1 and λ_2 are constants to be determined. As pointed out in Section II, exact system equilibriums cannot be obtained in advance. Hence, we use nominal system parameters to calculate the estimation $\hat{x}_i^*$ of the actual desired x_i^*. In the nominal case, the system runs on a flat ground, i.e., $\alpha = 0$, the estimation $\hat{x}_i^*$ is, therefore, given by

$$\hat{x}_3^* = 0, \qquad \hat{x}_2^* = x_2^*, \qquad \hat{G}_b \sin \hat{x}_1^* = \hat{D}_w \hat{x}_2^*. \tag{6}$$

The state trajectories can be driven to the sliding surface by choosing the control law τ such that

$$s\dot{s} \le -\eta\,|s| \tag{7}$$

where η is a positive constant.

From (3), it follows that

$$M_1(\mathbf{x})\dot{x}_2 + M_2(\mathbf{x})\dot{x}_3 = -D_w x_2 + G_b \sin x_1 + m_{12}x_3^2 \sin(x_1+\alpha) - \tilde{M} \tag{8}$$

where

$$M_1(\mathbf{x}) = m_{11} + m_{12}\cos(x_1+\alpha)$$
$$M_2(\mathbf{x}) = m_{22} + m_{12}\cos(x_1+\alpha). \tag{9}$$

From (8), we can rewrite (3) as follows:

$$\begin{cases} \dot{x}_1 = x_3 \\ \bar{M}(\mathbf{x})\dot{x}_2 + b(\mathbf{x}) = M_2(\mathbf{x})\tau \\ \bar{M}(\mathbf{x})\dot{x}_3 + a(\mathbf{x}) = -M_1(\mathbf{x})\tau \end{cases} \tag{10}$$

where

$$\bar{M}(\mathbf{x}) = m_{11}m_{22} - (m_{12}\cos(x_1+\alpha))^2$$
$$\begin{aligned} a(\mathbf{x}) = &-[m_{12}(D_b + D_w)\cos(x_1+\alpha) + m_{11}D_b]\,x_2 \\ &+ (m_{11} + m_{12}\cos(x_1+\alpha))\,D_b x_3 \\ &+ (m_{12}x_3)^2\cos(x_1+\alpha)\sin(x_1+\alpha) \\ &- m_{11}G_b \sin x_1 - m_{12}\cos(x_1+\alpha)\,\tilde{M} \end{aligned}$$
$$\begin{aligned} b(\mathbf{x}) = &[m_{22}(D_b + D_w) + m_{12}D_b\cos(x_1+\alpha)]\,x_2 \\ &- (m_{22} + m_{12}\cos(x_1+\alpha))\,D_b x_3 \\ &- m_{12}m_{22}x_3^2\sin(x_1+\alpha) \\ &+ m_{12}G_b \sin x_1 \cos(x_1+\alpha) + m_{22}\tilde{M}. \end{aligned}$$

Note that the function $\bar{M}(\mathbf{x})$ is positive because it is the determinant of the positive-definite matrix of the kinetic energy [25].

Let us define

$$f_1(\mathbf{x}) = \frac{a(\mathbf{x}) + \lambda_2 b(\mathbf{x})}{\bar{M}(\mathbf{x})}, \qquad \hat{f}_1(\mathbf{x}) = \frac{\hat{a}(\mathbf{x}) + \lambda_2 \hat{b}(\mathbf{x})}{\hat{\bar{M}}(\mathbf{x})} \tag{11}$$

and the estimation error that was caused by modeling uncertainty and disturbances is assumed to be bounded by some known function $F_1(\mathbf{x})$, which is given by

$$\left|f_1(\mathbf{x}) - \hat{f}_1(\mathbf{x})\right| \le F_1(\mathbf{x}). \tag{12}$$

Further, we assume that

$$\frac{\lambda_2 M_2(\mathbf{x}) - M_1(\mathbf{x})}{\bar{M}(\mathbf{x})} = (1+\Delta)\frac{\lambda_2 \hat{M}_2(\mathbf{x}) - \hat{M}_1(\mathbf{x})}{\hat{\bar{M}}(\mathbf{x})}$$
$$|\Delta| \le \beta_1 < 1. \tag{13}$$

Theorem 1: The achievement of a sliding motion on the surface (5) can be guaranteed by the selection of the control law

$$\tau = \frac{1}{\lambda_2 \hat{M}_2(\mathbf{x}) - \hat{M}_1(\mathbf{x})}\left(\hat{a}(\mathbf{x}) + \lambda_2 \hat{b}(\mathbf{x})\right) - \frac{\lambda_1 \hat{\bar{M}}(\mathbf{x})}{\lambda_2 \hat{M}_2(\mathbf{x}) - \hat{M}_1(\mathbf{x})}x_3 + \frac{\hat{\bar{M}}(\mathbf{x})}{\lambda_2 \hat{M}_2(\mathbf{x}) - \hat{M}_1(\mathbf{x})}k(\mathbf{x})\mathrm{sgn}(s) \tag{14}$$

where

$$k(\mathbf{x}) \le -\frac{F_1(\mathbf{x}) + \beta_1\,|r(\mathbf{x})| + \eta}{1-\beta_1}, \qquad r(\mathbf{x}) = \hat{f}_1(\mathbf{x}) - \lambda_1 \dot{x}_1. \tag{15}$$

Proof: Using the equivalent control method, the equivalent control law $\hat{\tau}$ can be easily obtained as follows:

$$\hat{\tau} = \frac{1}{\lambda_2 \hat{M}_2(\mathbf{x}) - \hat{M}_1(\mathbf{x})}\left(\hat{a}(\mathbf{x}) + \lambda_2 \cdot \hat{b}(\mathbf{x})\right) - \frac{\lambda_1 \hat{\bar{M}}(\mathbf{x})}{\lambda_2 \hat{M}_2(\mathbf{x}) - \hat{M}_1(\mathbf{x})}x_3 \tag{16}$$

Choosing the sliding-control law τ as $\tau = \hat{\tau} + \Delta\tau$, the rest of the work is to find appropriate switching control law $\Delta\tau$.

From (5), (10), and (16), the derivative of s is given by

$$\begin{aligned}\dot{s} &= \lambda_1\dot{x}_1 + \lambda_2\dot{x}_2 + \dot{x}_3 \\ &= \lambda_1\dot{x}_1 + \lambda_2\left(-\frac{b(\mathbf{x})}{\bar{M}(\mathbf{x})} + \frac{M_2(\mathbf{x})(\hat{\tau}+\Delta\tau)}{\bar{M}(\mathbf{x})}\right) \\ &\quad + \left(-\frac{a(\mathbf{x})}{\bar{M}(\mathbf{x})} - \frac{M_1(\mathbf{x})(\hat{\tau}+\Delta\tau)}{\bar{M}(\mathbf{x})}\right) \\ &= \lambda_1\dot{x}_1 + \frac{1}{\bar{M}(\mathbf{x})}\left[-a(\mathbf{x}) - \lambda_2 b(\mathbf{x}) + \lambda_2 M_2(\mathbf{x})\hat{\tau} - M_1(\mathbf{x})\hat{\tau}\right] \\ &\quad + \left(\frac{\lambda_2 M_2(\mathbf{x}) - M_1(\mathbf{x})}{\bar{M}(\mathbf{x})}\right)\Delta\tau \\ &= \frac{1}{\bar{M}(\mathbf{x})}\left\{\frac{\lambda_2 M_2(\mathbf{x}) - M_1(\mathbf{x})}{\lambda_2\hat{M}_2(\mathbf{x}) - \hat{M}_1(\mathbf{x})}\left[\hat{a}(\mathbf{x}) + \lambda_2\hat{b}(\mathbf{x})\right]\right. \\ &\quad \left. - \left[a(\mathbf{x}) + \lambda_2 b(\mathbf{x})\right]\right\} \\ &\quad - \left(\frac{\hat{\bar{M}}(\mathbf{x})}{\bar{M}(\mathbf{x})}\cdot\frac{\lambda_2 M_2(\mathbf{x}) - M_1(\mathbf{x})}{\lambda_2\hat{M}_2(\mathbf{x}) - \hat{M}_1(\mathbf{x})} - 1\right)\lambda_1\dot{x}_1 \\ &\quad + \left(\frac{\lambda_2 M_2(\mathbf{x}) - M_1(\mathbf{x})}{\bar{M}(\mathbf{x})}\right)\Delta\tau \\ &= \left(\hat{f}_1(\mathbf{x}) - f_1(\mathbf{x})\right) + \Delta\left(\hat{f}_1(\mathbf{x}) - \lambda_1\dot{x}_1\right) \\ &\quad + \left(\frac{\lambda_2 M_2(\mathbf{x}) - M_1(\mathbf{x})}{\bar{M}(\mathbf{x})}\right)\Delta\tau. \end{aligned} \tag{17}$$

Let us choose

$$\Delta\tau = \frac{\hat{\bar{M}}(\mathbf{x})}{\lambda_2\hat{M}_2(\mathbf{x}) - \hat{M}_1(\mathbf{x})}k(\mathbf{x})\mathrm{sgn}(s) \tag{18}$$

where $k(\mathbf{x})$ is a state-dependent function, and sgn$(\cdot)$ is the signum function. Note that $k(\mathbf{x})$ is always negative. Because inequality $1 - \beta_1 \le \Delta + 1$ holds, it follows that

$$\begin{aligned} s\dot{s} &= s\left[\left(\hat{f}_1(\mathbf{x}) - f_1(\mathbf{x})\right) + \Delta\cdot r(\mathbf{x}) + (\Delta+1)\,k(\mathbf{x})\mathrm{sgn}(s)\right] \\ &\le |s|\left(F_1(\mathbf{x}) + \beta_1\,|r(\mathbf{x})| + (1-\beta_1)\,k(\mathbf{x})\right). \end{aligned} \tag{19}$$

If $k(\mathbf{x})$ has the bound that is defined by (15), then the sliding condition (7) is satisfied. □

B. Surface-Stability Analysis

The controller (14) ensures that all system trajectories will reach the surface, and it remains there in the presence of model uncertainties and disturbances. The next step is to find appropriate coefficients λ_1 and λ_2 that guarantee the trajectories to be asymptotically stable during the sliding phase. On the sliding surface, the closed-loop system dynamics is represented by the combination of the sliding surface in the form $s = 0$ and (8)

$$\dot{x}_1 = x_3 \tag{20a}$$

$$M_1(\mathbf{x})\dot{x}_2 + M_2(\mathbf{x})\dot{x}_3 = -D_w x_2 + G_b\sin x_1 + m_{12}x_3^2\sin(x_1+\alpha) - \tilde{M} \tag{20b}$$

$$\lambda_1\left(x_1 - \hat{x}_1^*\right) + \lambda_2\left(x_2 - \hat{x}_2^*\right) + x_3 = 0. \tag{20c}$$

To avoid the confusion of notations, we use $\bar{\mathbf{x}}^* = [\,\bar{x}_1^* \quad \bar{x}_2^* \quad \bar{x}_3^*\,]^T$ to denote the real equilibrium of system (20), which is given by

$$\begin{aligned} \bar{x}_3^* = 0, \qquad & \lambda_1\left(\bar{x}_1^* - \hat{x}_1^*\right) + \lambda_2\left(\bar{x}_2^* - \hat{x}_2^*\right) = 0 \\ & G_b\sin\bar{x}_1^* = D_w\bar{x}_2^* + \tilde{M}. \end{aligned} \tag{21}$$

If the closed-loop system is asymptotically stable, then it will finally converge to $\bar{\mathbf{x}}^*$. It should be noted that usually the values of three kinds of equilibriums, i.e., $\mathbf{x}^*$, $\hat{\mathbf{x}}^*$, and $\bar{\mathbf{x}}^*$, are different because they are determined by different equations (4), (6), and (21), respectively.

Theorem 2: For the MWIP system (3), let us design the sliding surface (5) and control law (14). Let us assume that inequalities $M_1(\bar{\mathbf{x}}^*),\ M_2(\bar{\mathbf{x}}^*) > 0$ and $\cos(\bar{x}_1^*) > 0$ hold. If coefficients λ_1 and λ_2 satisfy

$$\lambda_1,\ \lambda_2 > 0, \qquad \lambda_2 M_2(\bar{\mathbf{x}}^*) - M_1(\bar{\mathbf{x}}^*) < 0 \tag{22}$$

then the closed-loop system is locally asymptotically stable around the equilibrium $\bar{\mathbf{x}}^*$.

Proof: From (20a) and (20c), we have

$$\begin{cases} x_2 = \left[-\lambda_1 x_1 - \dot{x}_1 + \lambda_1\hat{x}_1^* + \lambda_2\hat{x}_2^*\right]/\lambda_2 \\ \dot{x}_2 = \left(-\lambda_1\dot{x}_1 - \ddot{x}_1\right)/\lambda_2. \end{cases} \tag{23}$$

By substituting (23) into (20b) and introducing a new state vector

$$\mathbf{y} = [\,y_1 \quad y_2\,]^T = [\,x_1 \quad \dot{x}_1\,]^T \tag{24}$$

a new system is derived as follows:

$$\dot{\mathbf{y}} = \mathbf{\Phi}(\mathbf{y}) \tag{25}$$

where

$$\begin{aligned} \mathbf{\Phi}(\mathbf{y}) &= \begin{bmatrix}\Phi_1(\mathbf{y}) \\ \Phi_2(\mathbf{y})\end{bmatrix}, \qquad \Phi_1(\mathbf{y}) = y_2 \\ \Phi_2(\mathbf{y}) &= \frac{1}{\lambda_2 M_2(\mathbf{y}) - M_1(\mathbf{y})} \\ &\quad \times\left[\left(\lambda_1 M_1(\mathbf{y}) + D_w\right)y_2 + \lambda_2 m_{12}y_2^2\sin(y_1+\alpha)\right. \\ &\quad \left. + \lambda_1 D_w y_1 + \lambda_2 G_b\sin y_1 - D_w\left(\lambda_1\hat{x}_1^* + \lambda_2\hat{x}_2^*\right) - \lambda_2\tilde{M}\right]. \end{aligned} \tag{26}$$

It is apparent that system (20) and (25) are equivalent in terms of stability. The equilibrium of (25) is denoted by $\mathbf{y}^* = [\,y_1^* \quad y_2^*\,]^T = [\,\bar{x}_1^* \quad \bar{x}_3^*\,]^T$. As Ashrafiuon did in [20] and [21], we linearize (25) for the equilibrium $\mathbf{y}^*$ to establish linear stability criteria that guarantee local exponential stability of the nonlinear system. The linearized system is described by

$$\dot{\mathbf{y}} = \mathbf{A}\cdot\mathbf{y} \tag{27}$$

where

$$\mathbf{A} = \left.\frac{\partial\mathbf{\Phi}}{\partial\mathbf{y}}\right|_{\mathbf{y}^*} = \begin{bmatrix}0 & 1 \\ \Delta_1 & \Delta_2\end{bmatrix}, \quad \Delta_1 = \left.\frac{\partial\Phi_2}{\partial y_1}\right|_{\mathbf{y}^*}, \quad \Delta_2 = \left.\frac{\partial\Phi_2}{\partial y_2}\right|_{\mathbf{y}^*}. \tag{28}$$

The characteristic polynomial for the eigenvalues of matrix $\mathbf{A}$ is represented in the Laplace domain as follows:

$$|S\mathbf{I} - \mathbf{A}| = S^2 - \Delta_2 S - \Delta_1 = 0 \tag{29}$$

where S is the Laplace variable. According to the Hurwitz stability criteria, the equilibrium of the linearized system (27) is asymptotically stable, if we have

$$\Delta_1,\ \Delta_2 < 0. \tag{30}$$

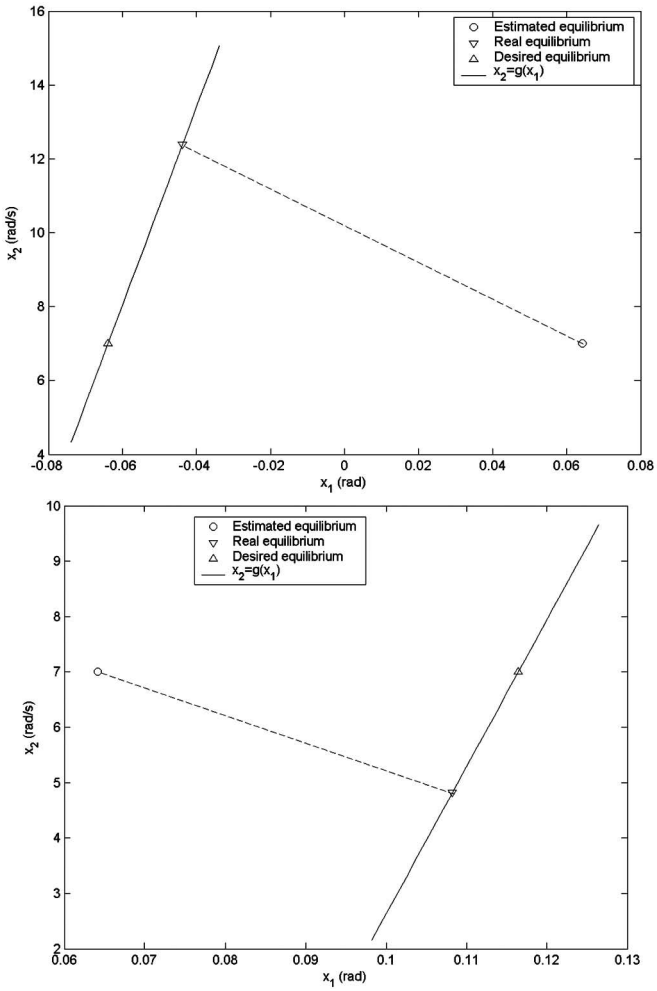

Fig. 2. Two possible distributions of three kinds of equilibriums when desired velocity is 7 rad/s.

After computation of the two derivatives in (28), we have

$$\Delta_1 = \frac{\lambda_1 D_w + \lambda_2 G_b \cos y_1^*}{\lambda_2 M_2(\mathbf{y}^*) - M_1(\mathbf{y}^*)}, \qquad \Delta_2 = \frac{\lambda_1 M_1(\mathbf{y}^*) + D_w}{\lambda_2 M_2(\mathbf{y}^*) - M_1(\mathbf{y}^*)}. \tag{31}$$

If we choose λ_1 and λ_2 that satisfy (22), inequality (30) is then satisfied. □

Because the MWIP system is required to move with a nearly upright body, the values of $M_1(\bar{\mathbf{x}}^*)$ and $M_2(\bar{\mathbf{x}}^*)$ are usually positive, if the slope angle is small enough. The value of $\cos(\bar{x}_1^*)$ is positive for the same reason. Hence, the assumptions of Theorem 2 are naturally satisfied. A difficulty in applying Theorem 2 is that it is hard to find proper coefficients λ_1 and λ_2 that satisfy the final inequality of (22), owing to unknown equilibrium $\bar{\mathbf{x}}^*$ and model uncertainties. In the practical situation, we can solve this problem by choosing a sufficiently small positive λ_2.

Fig. 2 shows two possible distributions of the three equilibriums in the $x_1 - x_2$ coordinate frame. Note that the real equilibrium $\bar{\mathbf{x}}^*$ is the intersection point of curve $x_2 = g(x_1) = (G_b/D_w)\sin(x_1) - \tilde{M}/D_w$ and a straight line crossing equilibrium $\hat{\mathbf{x}}^*$ with a slope $-\lambda_1/\lambda_2$. Although a steady tracking error $|\bar{x}_2^* - x_2^*|$ cannot be eliminated, it can be reduced to some extent by decreasing $|\lambda_1/\lambda_2|$.

IV. Design of the Second Sliding-Mode-Control Controller

When the first SMC controller is used, the real equilibrium $\bar{\mathbf{x}}^*$ is usually different from the desired equilibrium $\mathbf{x}^*$, even if the closed-loop system is asymptotically stable. This leads to a steady tracking error in the case of velocity control for the MWIP systems. To ensure that an MWIP system can move at a desired velocity $\dot{\theta}_w^*$, a novel sliding surface and the corresponding SMC-controller-design scheme is proposed in this section.

A. Sliding-Mode Controller Design

We start by introducing a new state vector

$$\mathbf{z} = [\, z_1 \quad z_2 \quad z_3 \quad z_4 \,]^T = [\, \theta_b \quad \dot{\theta}_b \quad \theta_w - \dot{\theta}_w^* t \quad \dot{\theta}_w - \dot{\theta}_w^* \,]^T. \tag{32}$$

The new sliding surface is given by

$$s = \mu_1 z_1 + z_2 + \mu_2 z_3 + \mu_3 z_4 \tag{33}$$

where coefficients $\mu_1,\ \mu_2,$ and μ_3 are constants to be determined.

Let us define

$$f_2(\mathbf{x}) = \frac{a(\mathbf{x}) + \mu_3 b(\mathbf{x})}{\bar{M}(\mathbf{x})}, \qquad \hat{f}_2(\mathbf{x}) = \frac{\hat{a}(\mathbf{x}) + \mu_3 \hat{b}(\mathbf{x})}{\hat{\bar{M}}(\mathbf{x})} \tag{34}$$

and the estimation error caused by modeling uncertainty and disturbances is assumed to be bounded by some known function $F_2(\mathbf{x})$, which is given by

$$\left| f_2(\mathbf{x}) - \hat{f}_2(\mathbf{x}) \right| \le F_2(\mathbf{x}). \tag{35}$$

Further, we assume that

$$\frac{\mu_3 M_2(\mathbf{x}) - M_1(\mathbf{x})}{\bar{M}(\mathbf{x})} = (1 + \tilde{\Delta}) \frac{\mu_3 \hat{M}_2(\mathbf{x}) - \hat{M}_1(\mathbf{x})}{\hat{\bar{M}}(\mathbf{x})}$$

$$\left| \tilde{\Delta} \right| \le \beta_2 < 1. \tag{36}$$

The second SMC controller is proposed by the following theorem.

Theorem 3: The achievement of a sliding motion on the surface (33) can be guaranteed by the selection of the control law

$$\tau = \frac{1}{\mu_3 \hat{M}_2(\mathbf{x}) - \hat{M}_1(\mathbf{x})} \left(\hat{a}(\mathbf{x}) + \mu_3 \cdot \hat{b}(\mathbf{x}) \right) - \frac{\mu_1 \hat{\bar{M}}(\mathbf{x})}{\mu_3 \hat{M}_2(\mathbf{x}) - \hat{M}_1(\mathbf{x})} z_2$$

$$- \frac{\mu_2 \hat{\bar{M}}(\mathbf{x})}{\mu_3 \hat{M}_2(\mathbf{x}) - \hat{M}_1(\mathbf{x})} z_4 + \frac{\hat{\bar{M}}(\mathbf{x})}{\mu_3 \hat{M}_2(\mathbf{x}) - \hat{M}_1(\mathbf{x})} \tilde{k}(\mathbf{x}) \mathrm{sgn}(s) \tag{37}$$

where $\hat{a}(\mathbf{x})$ and $\hat{b}(\mathbf{x})$ are the same, as described in Section III, and $\tilde{k}(\mathbf{x})$ and $\tilde{r}(\mathbf{x})$ satisfy

$$\tilde{k}(\mathbf{x}) \le -\frac{F_2 + \beta_2 |\tilde{r}(\mathbf{x})| + \eta}{1 - \beta_2}, \qquad \tilde{r}(\mathbf{x}) = \hat{f}_2(\mathbf{x}) - \mu_1 z_2 - \mu_2 z_4. \tag{38}$$

Proof: This theorem can be easily proven using the similar method given in the Proof of Theorem 1. □

B. Surface-Stability Analysis

A similar approach as used in Section III-B is assumed to analyze the stability of the sliding surface (33). By choosing a new state vector $\mathbf{q} = [\, q_1 \quad q_2 \quad q_3 \,]^T = [\, z_1 \quad z_2 \quad z_4 \,]^T$, the closed-loop system dynamics on the sliding surface (33) is represented by

$$\dot{q}_1 = q_2 \tag{39a}$$

$$M_1(\mathbf{q})\dot{q}_3 + M_2(\mathbf{q})\dot{q}_2 = -D_w \left(q_3 + \dot{\theta}_w^* \right) + G_b \sin q_1 + m_{12} q_2^2 \sin(q_1 + \alpha) - \tilde{M} \tag{39b}$$

$$\mu_1 q_2 + \dot{q}_2 + \mu_2 q_3 + \mu_3 \dot{q}_3 = 0. \tag{39c}$$

Equation (39) can be further transformed into the following vector form:

$$\dot{\mathbf{q}} = \mathbf{\Psi}(\mathbf{q}) \tag{40}$$

where

$$\mathbf{\Psi}(\mathbf{q}) = [\,\Psi_1(\mathbf{q}) \quad \Psi_2(\mathbf{q}) \quad \Psi_3(\mathbf{q})\,]^T$$

$$\Psi_1(\mathbf{q}) = q_2$$

$$\Psi_2(\mathbf{q}) = \frac{1}{\mu_3 M_2(\mathbf{q}) - M_1(\mathbf{q})} \left[\mu_1 M_1(\mathbf{q}) q_2 + (\mu_2 M_1(\mathbf{q}) - \mu_3 D_w)\, q_3 + \mu_3 m_{12} q_2^2 \sin(q_1 + \alpha) + \mu_3 G_b \sin q_1 - D_w \mu_3 \dot{\theta}_w^* - \mu_3 \tilde{M}\right]$$

$$\Psi_3(\mathbf{q}) = \frac{1}{\mu_3 M_2(\mathbf{q}) - M_1(\mathbf{q})} \left[-\mu_1 M_2(\mathbf{q}) q_2 - (\mu_2 M_2(\mathbf{q}) - D_w)\, q_3 - m_{12} q_2^2 \sin(q_1 + \alpha) - G_b \sin q_1 + D_w \dot{\theta}_w^* + \tilde{M}\right]. \tag{41}$$

Obviously, point $\mathbf{q}^* = [\,x_1^* \quad 0 \quad 0\,]$ is one of the equilibriums of the nonlinear system (40), where x_1^* is the real desired inclination body angle, which is determined by (4). Our aim is to choose suitable coefficients μ_1, μ_2, and μ_3 that guarantee the asymptotical stability of this equilibrium.

Theorem 4: For the MWIP system (3), let us design sliding surface (33) and control law (37). Let us assume that inequalities $M_1(\mathbf{q}^*)$, $M_2(\mathbf{q}^*) > 0$ and $\cos(x_1^*) > 0$ hold, if coefficients μ_1, μ_2, and μ_3 satisfy

$$\begin{aligned} &\mu_1 M_1(\mathbf{q}^*) + D_w > \mu_2 M_2(\mathbf{q}^*) \\ &\mu_3 M_2(\mathbf{q}^*) - M_1(\mathbf{q}^*) < 0 \\ &\mu_1, \mu_2, \mu_3 > 0, \qquad \mu_1 \mu_3 > \mu_2 \end{aligned} \tag{42}$$

then the closed-loop system is locally asymptotically stable around the equilibrium $\mathbf{q}^*$.

Proof: We linearize (41) for the equilibrium $\mathbf{q}^*$ to establish linear stability criteria that guarantee local exponential stability of the nonlinear system. The linearized system is described by

$$\dot{\mathbf{q}} = \mathbf{B} \cdot (\mathbf{q} - \mathbf{q}^*) \tag{43}$$

where

$$\mathbf{B} = \left.\frac{\partial \mathbf{\Psi}}{\partial \mathbf{q}}\right|_{\mathbf{q}^*} = \begin{bmatrix} 0 & 1 & 0 \\ \Delta_1 & \Delta_2 & \Delta_3 \\ \Delta_4 & \Delta_5 & \Delta_6 \end{bmatrix} \tag{44}$$

$$\Delta_1 = \left.\frac{\partial \Psi_2}{\partial q_1}\right|_{\mathbf{q}^*}, \qquad \Delta_2 = \left.\frac{\partial \Psi_2}{\partial q_2}\right|_{\mathbf{q}^*}, \qquad \Delta_3 = \left.\frac{\partial \Psi_2}{\partial q_3}\right|_{\mathbf{q}^*}$$

$$\Delta_4 = \left.\frac{\partial \Psi_3}{\partial q_1}\right|_{\mathbf{q}^*}, \qquad \Delta_5 = \left.\frac{\partial \Psi_3}{\partial q_2}\right|_{\mathbf{q}^*}, \qquad \Delta_6 = \left.\frac{\partial \Psi_3}{\partial q_3}\right|_{\mathbf{q}^*}. \tag{45}$$

According to the Hurwitz stability criteria, the equilibrium of the linearized system (43) is asymptotically stable, if we have

$$\begin{aligned} &\Delta_2 + \Delta_6 < 0, \qquad \Delta_1 \Delta_6 - \Delta_3 \Delta_4 > 0 \\ &(\Delta_2 + \Delta_6)(\Delta_3 \Delta_5 - \Delta_2 \Delta_6) + \Delta_1 \Delta_2 + \Delta_3 \Delta_4 > 0. \end{aligned} \tag{46}$$

It follows from (41) and (45) that

$$\begin{aligned} \Delta_2 + \Delta_6 &= -\mu_1 \delta^* M_1(\mathbf{q}^*) + \mu_2 \delta^* M_2(\mathbf{q}^*) - \delta^* D_w \\ \Delta_1 \Delta_6 - \Delta_3 \Delta_4 &= \mu_2 \delta^* G_b \cos x_1^* \\ \Delta_3 \Delta_5 - \Delta_2 \Delta_6 &= (\delta^*)^2 \mu_1 D_w (\mu_3 M_2(\mathbf{q}^*) - M_1(\mathbf{q}^*)) \\ \Delta_1 \Delta_2 + \Delta_3 \Delta_4 &= (\delta^*)^2 G_b \cos x_1^* [(\mu_1 \mu_3 - \mu_2) M_1(\mathbf{q}^*) + \mu_3 D_w] \end{aligned} \tag{47}$$

TABLE I
EXACTLY KNOWN PHYSICAL PARAMETERS OF THE MWIP SYSTEM

Mass of the wheel (Kg)	Moment of inertia of the wheel (Kg.m^2)	Radius of the wheel (m)	Length between the wheel axle and the center of gravity of the body (m)
$m_w = 29.0$	$I_w = 0.6$	$r = 0.254$	$l = 0.267$

TABLE II
UNCERTAIN BODY PARAMETERS OF THE MWIP SYSTEM

	Mass of the body (Kg)	Moment of inertia of the body (Kg.m^2)
Actual system	$m_b = 310.6$	$I_b = 65.0$
Nominal system	$\hat{m}_b = 137.6$	$\hat{I}_b = 35.0$

where δ^* is given by

$$\delta^* = \frac{1}{M_1(\mathbf{q}^*) - \mu_3 M_2(\mathbf{q}^*)}. \tag{48}$$

Apparently, inequalities (46) hold if coefficients μ_1, μ_2, and μ_3 are chosen to satisfy (42). This completes the proof. □

Note that the problem of uncertain equilibriums is solved by using a special sliding surface (33). The third term given in the right-hand side of (33) plays an important role in avoiding uncertain equilibriums. In fact, state z_3 is the integration of state z_4, which can eliminate the static tracking error, like an integral part, in a commonly used proportional–integral–derivative controller.

V. SIMULATION STUDY

Let us consider an MWIP system, whose exactly known system parameters are listed in Table I. To test the robustness of the proposed controllers, it is assumed that the actual physical parameters of the body are different from that of the nominal system. Table II shows the actual and nominal body parameters. The dissipation parameters D_w and D_b and the measurement noises are assumed to be Gaussian random variables with known covariance and mean values. To demonstrate the robustness of the proposed SMC controllers with respect to the external disturbances, we applied an external torque τ_1 to the body of the MWIP system from time 15 to 16 s. This torque is also thought as a Gaussian random variable, which is used to simulate a disturbance coming from the wind. All the mean and covariance values of aforementioned random variables are shown in Table III. A linear-quadratic regulator controller designed by linearizing nominal system was found that cannot stabilize the actual system.

A. Simulation Study for the First Sliding-Mode-Control Controller

The function $F_1(\mathbf{x})$, given in (12), the parameter β_1, and η were selected as $0.1 \times \left|\hat{f}_1(\mathbf{x})\right|$, 0.1, and 1, respectively. Function $k(\mathbf{x})$ was given by

$$k(\mathbf{x}) = \frac{-\left(F_1(\mathbf{x}) + \beta_1 |r(\mathbf{x})| + \eta\right)}{1 - \beta_1} - 1.$$

Let us assume that the desired moving velocity is $x_2^* = \dot{\theta}_w^* = 7$ rad/s. From (6), we can compute the estimated equilibrium $\hat{\mathbf{x}}^*$, which is used to construct the initial sliding surface (5). Therefore, the final

TABLE III
GAUSSIAN RANDOM VARIABLES IN THE SIMULATION

	Mean	Covariance
D_w (N.s/m)	3.3	1.0
D_b (N.s/m)	0.1	0.03
Measurement noise of θ_b (rad)	0.0	0.01
Measurement noise of $\dot{\theta}_w$ (rad/s)	0.0	0.01
Measurement noise of $\dot{\theta}_b$ (rad/s)	0.0	0.01
τ_1 (N.m)	20.0	1.0

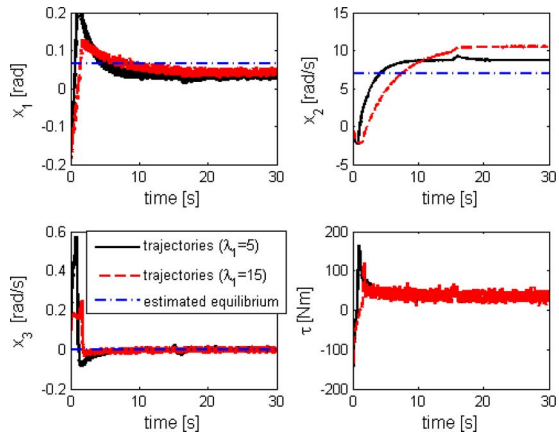

Fig. 3. System trajectories by using the first SMC controller.

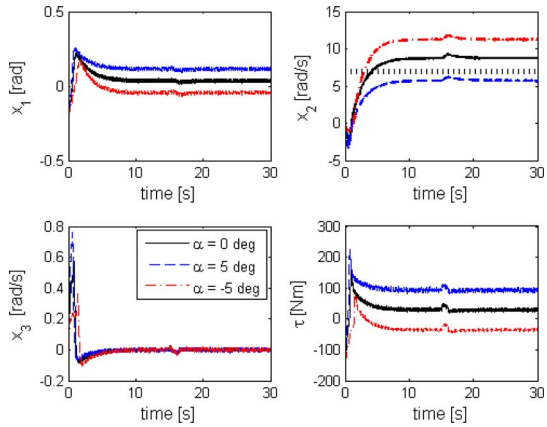

Fig. 4. System trajectories using the first SMC controller on different slopes. (Black dot line denotes the desired velocity.)

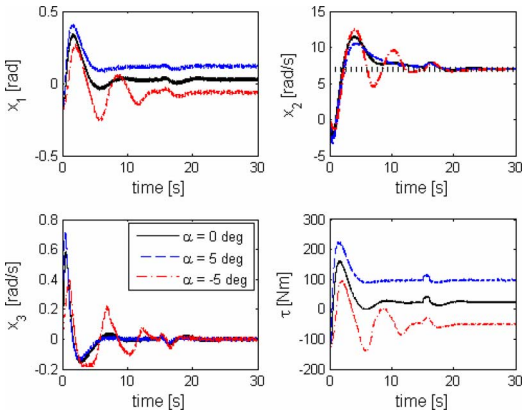

Fig. 5. System trajectories using the second SMC controller on different slopes. (Black dot line denotes the desired velocity.)

SMC controller (14) can be obtained from Theorem 2 by selecting appropriate λ_1 and λ_2. In order to avoid chattering associated with the sliding-mode control law, we have approximated the discontinuous signum function (sgn(s)) with continuous saturation function of small boundary layers.

To analyze the effect of coefficients λ_1 and λ_2, we first investigated the simulation by using two SMC controllers with different combination of λ_1 and λ_2. In both cases, coefficient λ_2 was equal to 0.1, and coefficient λ_1 was selected as $\lambda_1 = 5$ and $\lambda_1 = 15$, respectively. Suppose that the initial condition of the system is $\mathbf{x}(0) = [-0.175 \quad 0 \quad 0]$ and that the slope of ground is $\alpha = 0°$. Fig. 3 shows the system state and control input trajectories of these two cases by using the first SMC controller. The system is asymptotically stable, even when there are parameter uncertainties and external disturbances, whereas steady tracking errors are inevitable in both cases. Note that the steady tracking error can be remarkably reduced by selecting smaller coefficient λ_1. At the same time, faster convergence speed can also be obtained. These results are coincident with the theoretical conclusions given in Theorem 2. Nevertheless, the better performance brought by smaller coefficient λ_1 leads to a higher peak value of the body inclination angle x_1, which may make the passenger to feel fearsome. Note that when the first SMC controller is used, there is an unavoidable velocity-tracking error, even if the MWIP system runs on flat ground.

To further validate the robustness of the first SMC controller, we performed the velocity-control simulation of an MWIP system on different slopes. Three different cases of ground slope, i.e., $\alpha = 0°$, $\alpha = 5°$ and $\alpha = -5°$, were considered in the simulation. The simulation results are shown in Fig. 4. In all cases, the system was stabilized, while the modeling uncertainties and external disturbance exist. Note that there are unavoidable steady tracking errors in all the three cases.

B. Simulation Study for the Second Sliding-Mode-Control Controller

The function $F_2(\mathbf{x})$, given in (35), the parameter β_2, and η were selected as $0.1 \times \left|\hat{f}_2(\mathbf{x})\right|$, 0.1, and 1, respectively. Function $\tilde{k}(\mathbf{x})$ was given by

$$\tilde{k}(\mathbf{x}) = \frac{-\left(F_2(\mathbf{x}) + \beta_2 \left|\tilde{r}(\mathbf{x})\right| + \eta\right)}{1 - \beta_2} - 1.$$

Let us assume that the desired moving velocity is $x_2^* = \dot{\theta}_w^* = 7\,\mathrm{rad/s}$. According to Theorem 4, coefficients μ_1, μ_2, and μ_3 were selected as $\mu_1 = 1.5$, $\mu_2 = 0.01$, and $\mu_3 = 0.05$. Three different cases of ground slope, i.e., $\alpha = 0°$, $\alpha = 5°$, and $\alpha = -5°$, were also assumed.

The final simulation results by using the second SMC controller are depicted in Fig. 5. In all the three cases, the MWIP system is asymptotical stable with very small steady tracking error, which substantiates the efficiency of the presented approach. If the physical parameters of an MWIP system are very close to those of the nominal system, then the maximum slope that we achieved in the simulation is about 45°. This also demonstrates the robustness of the proposed approach.

Compared with the first SMC controller, the most significant advantage of the second SMC controller is its ability to eliminate the

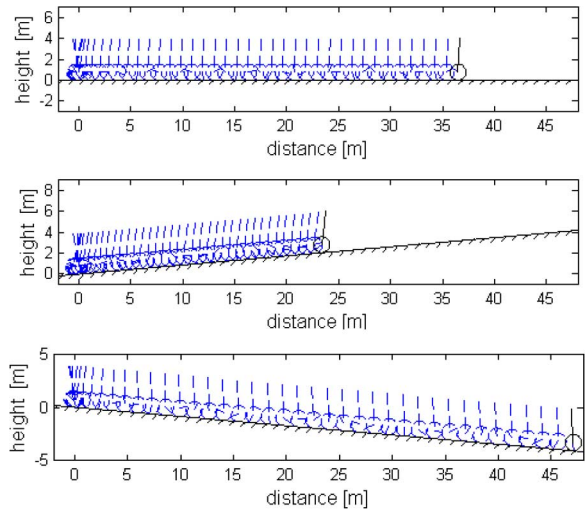

Fig. 6. Animations of the simulation when $\alpha = 0^\circ$, $\alpha = 5^\circ$, and $\alpha = -5^\circ$ (from 0 to 20 s, using the first SMC controller).

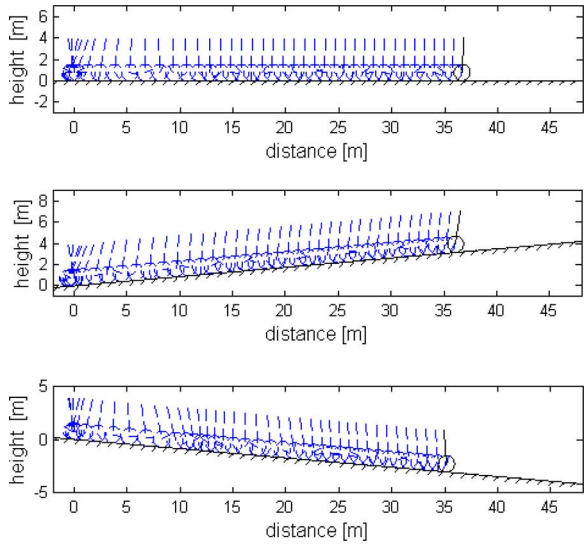

Fig. 7. Animations of the simulation when $\alpha = 0^\circ$, $\alpha = 5^\circ$, and $\alpha = -5^\circ$ (from 0 to 20 s, using the second SMC controller).

steady tracking error. Nevertheless, the system transient behavior by using the second SMC controller seems to be more complicated than the other. For instance, overshoot occurred in all the three cases shown by Fig. 5. This might be caused by the higher order dynamics (40) near the equilibrium. As a result, it is more difficult to obtain a satisfactory transient behavior when using the second SMC controller, since more coefficients need to be adjusted.

The animations corresponding to Figs. 4 and 5 are shown in Figs. 6 and 7, respectively. These animations provide an intuitive feel to drive an MWIP system by using the two proposed SMC controllers. Except the initial phase, the system runs smoothly and stably. When using the first SMC controller in the three slopes, the distances that the system passed during a same time interval are much different due to the different steady velocity. This way, the second SMC controller performs better, as shown in Fig. 7.

VI. Conclusion

The robust velocity-tracking control problem of the mobile-wheeled inverted-pendulum models has been investigated in this study. Sliding-mode control method has been chosen due to its robustness to nonlinear systems. Normally, it is hard to design an SMC controller for general underactuated mechanical systems. In our special case, we proposed two SMC controllers for the mobile-wheeled inverted pendulum considering both parameter uncertainties and external disturbance. The first SMC controller can robustly stabilize the MWIP system, while the parameter uncertainties cause uncertain equilibrium in a velocity-control problem, which brings unavoidable tracking error. The second SMC controller can eliminate the steady tracking error with the use of a special sliding surface. The efficiency of the proposed two SMC controllers is confirmed by numerical simulations. In all the simulations, both of the proposed SMC controllers are able to stabilize the MWIP system, while there are parameter uncertainties and external disturbances. This study might be the first attempt to solve the set-point velocity-control problem with uncertain equilibrium, which is an interesting phenomena to control the underactuated systems. To the best of our knowledge, previous methods might be not able to deal with this problem. Future research would be to apply the proposed controllers in a real MWIP system.

Appendix
Derivation of an MWIP System Model

The coordinate frame of an MWIP system on a slope is shown in Fig. 1. The positions and velocities of the wheel and the body can be given by

$$\begin{cases} x_b = l\sin\theta_b + r\theta_w\cos\alpha \\ y_b = l\cos\theta_b + r\theta_w\sin\alpha \end{cases} \tag{A1}$$

$$\begin{cases} x_w = r\theta_w\cos\alpha \\ y_w = r\theta_w\sin\alpha \end{cases} \tag{A2}$$

$$\begin{cases} \dot{x}_b = l\dot{\theta}_b\cos\theta_b + r\dot{\theta}_w\cos\alpha \\ \dot{y}_b = -l\dot{\theta}_b\sin\theta_b + r\dot{\theta}_w\sin\alpha \end{cases} \tag{A3}$$

$$\begin{cases} \dot{x}_w = r\dot{\theta}_w\cos\alpha \\ \dot{y}_w = r\dot{\theta}_w\sin\alpha. \end{cases} \tag{A4}$$

The Larangian equation of motion is used for the derivation of the dynamic equation. The kinetic, potential, and dissipated energy and their contributions to the dynamic equation are computed as follows.

The kinetic energies of the body and the wheel can then be computed as follows:

$$\begin{aligned} V_b &= \frac{1}{2}m_b\left(\dot{x}_b^2 + \dot{y}_b^2\right) + \frac{1}{2}I_b\dot{\theta}_b^2 \\ &= \frac{1}{2}m_b\left(r^2\dot{\theta}_w^2 + 2rl\dot{\theta}_b\dot{\theta}_w\cos(\theta_b+\alpha) + l^2\dot{\theta}_b^2\right) + \frac{1}{2}I_b\dot{\theta}_b^2 \end{aligned} \tag{A5}$$

$$V_w = \frac{1}{2}m_w\left(\dot{x}_w^2 + \dot{y}_w^2\right) + \frac{1}{2}I_w\dot{\theta}_w^2 = \frac{1}{2}m_w r^2\dot{\theta}_w^2 + \frac{1}{2}I_w\dot{\theta}_w^2. \tag{A6}$$

The gravitational potential energy of the body and the wheel can be computed as follows:

$$U_b = m_b g\left(l\cos\theta_b + r\theta_w\sin\alpha\right) \tag{A7}$$

$$U_w = m_w g r\theta_w\sin\alpha. \tag{A8}$$

Therefore, the Lagrange function L is given by

$$L = V_b + V_w - U_b - U_w\,. \tag{A9}$$

According to the Lagrange's motion equation, the dynamic model of an MWIP system can be represented by

$$\begin{aligned}\frac{d}{dt}\left(\frac{\partial L}{\partial \dot{\theta}_b}\right) - \frac{\partial L}{\partial \theta_b} &= -\tau - D_b\left(\dot{\theta}_b - \dot{\theta}_w\right)\\ \frac{d}{dt}\left(\frac{\partial L}{\partial \dot{\theta}_w}\right) - \frac{\partial L}{\partial \theta_w} &= \tau + D_b\left(\dot{\theta}_b - \dot{\theta}_w\right) - D_w\dot{\theta}_w\,.\end{aligned} \tag{A10}$$

It follows from (A10) that the final nonlinear model can be described by (1).

ACKNOWLEDGMENT

The authors would like to thank the Equos Research Co., Ltd. for their help in providing valuable simulation data of a real vehicle.

REFERENCES

[1] K. Pathak, J. Franch, and S. K. Agrawal, "Velocity and position control of a wheeled inverted pendulum by partial feedback linearization," *IEEE Trans. Robot.*, vol. 21, no. 3, pp. 505–513, Jun. 2005.
[2] A. Salerno and J. Angeles, "The control of semi-autonomous two-wheeled robots undergoing large payload-variations," in *Proc. IEEE Int. Conf. Robot. Autom.*, New Orleans, LA, 2004, pp. 1740–1745.
[3] Y.-S. Ha and S. Yuta, "Trajectory tracking control for navigation of the inverse pendulum type self-contained mobile robot," *Robot. Autonom. Syst.*, vol. 17, pp. 65–80, 1996.
[4] Y. Kim, S. H. Kim, and Y. K. Kwak, "Dynamic analysis of a nonholonomic two-wheeled inverted pendulum robot," *J. Intell. Robot. Syst.*, vol. 44, no. 1, pp. 25–46, 2005.
[5] T. J. Ren, T. C. Chen, and C. J. Chen, "Motion control for a two-wheeled vehicle using a self-tuning PID controller," *Control Eng. Practice*, vol. 16, no. 3, pp. 365–375, 2008.
[6] M. Baloh and M. Parent, "Modeling and model verification of an intelligent self-balancing two-wheeled vehicle for an autonomous urban transportation system," presented at the Conf. Comp. Intell., Robot. Autonom. Syst., Singapore, 2003.
[7] F. Grasser, A. D'Arrigo, S. Colombi, and A. Rufer, "Joe: A mobile, inverted pendulum," *IEEE Trans. Ind. Electron.*, vol. 49, no. 1, pp. 107–114, Feb. 2002.
[8] (2010). [Online]. Available: http://www.geology.smu.edu/∼dpa-www/robo/nbot/
[9] (2003). [Online]. Available: http://www.teamhassenplug.org/robots/legway/
[10] H. Tirmant, M. Baloh, L. Vermeiren, T. M. Guerra, and M. Parent, "B2, an alternative two wheeled vehicle for an automated urban transportation system," in *Proc. IEEE Intell. Veh. Symp.*, Paris, France, 2002, pp. 594–603.
[11] (2010). [Online]. Available: http://www.segway.com
[12] M. Karkoub and M. Parent, "Modelling and non-linear feedback stabilization of a two-wheel vehicle," *Proc. Inst. Mech. Eng., I: J. Syst. Control Eng.*, vol. 218, no. 8, pp. 675–686, 2004.
[13] M. W. Spong, "The swing up control problem for the acrobat," *IEEE Control Syst. Mag.*, vol. 15, no. 1, pp. 49–55, Feb. 1995.
[14] I. Fantoni, R. Lozano, and M. W. Spong, "Energy based control of the pendubot," *IEEE Trans. Autom. Control*, vol. 45, no. 4, pp. 725–729, Apr. 2000.
[15] Y.-L. Gu, "Direct adaptive control scheme for underactuated dynamic systems," in *Proc. IEEE Conf. Decision Control*, San Antonio, TX, 1993, pp. 1625–1627.
[16] A. M. Bloch, N. E. Leonard, and J. E. Marsden, "Stabilization of the pendulum on a rotor arm by the method of controlled Lagrangians," in *Proc. IEEE Int. Conf. Robot. Autom.*, Piscataway, NJ, 1999, pp. 500–505.
[17] M. Karkoub, "Modelling and robust μ-synthesis control of an intelligent self balancing two-wheel vehicle," *Proc. Inst. Mech. Eng., K: J. Multi-Body Dyn.*, vol. 220, no. 4, pp. 293–302, 2006.
[18] W. Wang, J. Yi, D. Zhao, and D. Liu, "Design of a stable sliding-mode controller for a class of second-order underactuated systems," *Proc. Inst. Electr. Eng.: Control Theory Appl.*, vol. 151, no. 6, pp. 683–690, 2004.
[19] B. L. Ma, "Comment on 'Design of a stable sliding-mode controller for a class of second-order underactuated systems,'" *IET Control Theory Appl.*, vol. 1, no. 4, pp. 1186–1187, 2007.
[20] H. Ashrafiuon and R. S. Erwin, "Sliding control approach to underactuated multibody systems," in *Proc. Amer. Control Conf.*, Boston, MA, 2004, pp. 1283–1288.
[21] M. Nikkhah, H. Ashrafiuon, and F. Fahimi, "Robust control of underactuated biped using sliding modes," *Robotica*, vol. 25, no. 3, pp. 367–374, 2006.
[22] K. Lee and V. Coverstone-Carroll, "Control algorithms for stabilizing underactuated robots," *J. Robot. Syst.*, vol. 15, no. 12, pp. 681–697, 1998.
[23] C.-Y. Su and Y. Stepanenko, "Sliding mode control of non-holonomic systems: Underactuated manipulator case," in *Proc. Int. Fed. Automat. Control Nonlinear Control Syst. Design*, Tahoe City, CA, 1995, pp. 609–613.
[24] J. Huang, H. W. Wang, T. Matsuno, T. Fukuda, and K. Sekiyama, "Robust velocity sliding mode control of mobile wheeled inverted pendulum systems," in *Proc. IEEE Int. Conf. Robot. Autom.*, Kobe, Japan, 2009, pp. 2983–2988.
[25] A. M. Formal'skii, "An inverted pendulum on a fixed and a moving base," *J. Appl. Math. Mech.*, vol. 70, pp. 56–64, 2006.
[26] O. Matsumoto, S. Kajita, and K. Tani, "Estimation and control of the attitude of a dynamic mobile robot using internal sensors," *Adv. Robot.*, vol. 7, no. 2, pp. 159–178, 1993.

Invariant Trajectory Tracking With a Full-Size Autonomous Road Vehicle

Moritz Werling, Lutz Gröll, and Georg Bretthauer

***Abstract*—Safe handling of dynamic inner-city scenarios with autonomous road vehicles involves the problem of stabilization of precalculated state trajectories. In order to account for the practical requirements of the holistic autonomous system, we propose two complementary nonlinear Lyapunov-based tracking-control laws to solve the problem for speeds between ± 6 m/s. Their designs are based on an extended kinematic one-track model, and they provide a smooth, singularity-free stopping transient. With regard to autonomous test applications, the proposed tracking law without orientation control performs much better with respect to control effort and steering-input saturation than the one with orientation control but needs to be prudently combined with the latter for backward driving. The controller performance is illustrated with a full-size test vehicle.**

***Index Terms*—Back-stepping, full-size autonomous road vehicle, invariant trajectory tracking, Lyapunov-based control, nonholonomic.**

I. INTRODUCTION

The past three decades have witnessed an ambitious research effort in the area of automated driving. This has led to a remarkable enhancement in terms of handling complex situations robustly. The

Manuscript received December 5, 2009; revised April 13, 2010; accepted June 1, 2010. Date of publication July 1, 2010; date of current version August 10, 2010. This paper was recommended for publication by Associate Editor W. Chung and Editor G. Oriolo upon evaluation of the reviewers' comments.

M. Werling is with the Department of Applied Computer Science and Automation, Karlsruhe Institute of Technology, 76128 Karlsruhe, Germany (e-mail: moritz.werling@kit.edu).

L. Gröll and G. Bretthauer are with the Department of Applied Computer Science, Karlsruhe Institute of Technology, 76344 Eggenstein-Leopoldshafen, Germany (e-mail: groell@iai.fzk.de; bretthauer@iai.fzk.de).

This paper has supplementary video material of the test runs available at http://ieeexplore.ieee.org.

Digital Object Identifier 10.1109/TRO.2010.2052325